Asian Journal of Chemistry; Vol. 37, No. 4 (2025), 851-857

ASIAN JOURNAL OF CHEMISTRY

https://doi.org/10.14233/ajchem.2025.33396

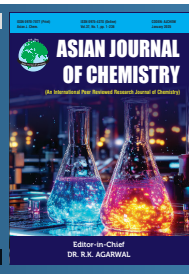

Synthesis, Characterization, Magnetic and Electrochemical Properties of Lithium Cobalt Ferrites: A High-Performance Materials for Lithium-Ion Batteries

G. Gowri Shanmugapriya, R. Rajikha, S. Analisa, S. Umamaheswari and V. Sathana*

PG & Research Department of Physics, St. Joseph's College of Arts & Science (Autonomous), Cuddalore-607001, India

*Corresponding author: E-mail: sathana@sjctnc.edu.in

Received: 21 January 2025; *Accepted*: 4 March 2025; *Published online*: 29 March 2025; AJC-21946

The lithium cobalt ferrite with different concentration, $Li_{0.75}Co_{(5+3x/8)}Fe_{2-y}O_4$ (x = 0, 1, 2, 3, 4) (y = 0, 0.25, 0.5, 0.75, 1) were synthesized by sol-gel process. The structural, morphological, magnetic and electrical properties were investigated with XRD, FESEM-EDS mapping, FTIR, VSM and impedance techniques. The addition of lithium, a reactive soft alkali metal, greatly improves the electrochemical conduction processes when it is blended with ferrite. The change from bulk ferrite to nanomaterials results in significant alterations to its physical, magnetic and electrical characteristics, substituting cobalt alters pure lithium ferrite into a magnetically active substance. The development of cubic structure in all the compounds was proved from X-ray diffraction analysis. The VSM results demonstrated that all prepared materials exhibit soft magnetic characteristics, with a squareness ratio (M_r/M_s) of less than 0.5. This indicates the presence of multi domain magnetic particles which are appropriate for use in transformer coils and cores, resulting in lower induction. The morphology and chemical composition of the composite were confirmed in FESEM and EDS mapping analysis. FTIR analysis shows metal-oxygen bonds (Fe-O, Co-O) confirmed the presence of lithium cobalt ferrite. From impedance studies, the electrochemical properties of the prepared compounds were analyzed. The dielectric parameters were examined using impedance analysis, revealing enhanced electrical conductivity and emphasizing the multifunctional characteristics of the synthesized material, which may render it applicable in diverse fields necessitating both magnetic and dielectric features.

Keywords: Nanomaterial, Sol-gel method, Magnetic nanoparticles, Lithium cobalt ferrite, Dielectric properties, Impedance.

INTRODUCTION

Advancement in nanotechnology involves discovering novel materials, synthesis methods and theoretical/experimental techniques [1,2]. Nanotechnology provides more than just super-ficial improvements to the existing technologies, but also it brings groundbreaking, transformative discoveries and innovations that can benefit to the society as well as environment. Creating new technologies and nanomaterials with tailored properties can lead to innovative products enhancing our living environment [3,4]. Ferrite nanoparticles, in particular, have garnered significant attention due to their vast applications in electronics, high-density magnetic storage, optics, targeted drug delivery systems, ceramics, magnetic resonance imaging contrast agents, transformer cores, catalysis in biomedicines, *etc*. [5-8].

The nanoscale ferrites, which exhibit distinct structural, physical, magnetic and electrical properties compared to bulk materials [9-12]. The unique properties of certain spinel transition metal oxides, such as ferrites, allow for the combination of magnetic characteristics and ion storage capabilities, enabling the development of adjustable devices that can be regulated by lithium ions [13,14]. Incorporating non-magnetic lithium ions enhances conductivity in nano-ferrites while maintaining electroneutrality [15,16]. Therefore, lithium ferrite, a metal spinel nanoparticle, offers various benefits [15,17,18]. Studies on the cobalt lithium ferrite reveals that increased lithium concentration leads to enhance the ionic mobility, reduced resistivity, increased ferrite formation [17,19,20]. Moreover, low electronegativity value of lithium increases, dielectric constant, tangent loss and AC conductivity [21,22].

Sol-gel method was employed for the synthesis due to its numerous advantages including ability to be carried out at ambient temperature [23], simple and straight forward fabrication procedure [24], production of high-quality materials at relatively low temperatures [25], capability to produce thin coatings, ensu-

ring excellent adhesion between the substrate and top layer, economical and efficient method for producing high-quality coverage, potential for producing novel and functional materials with applications in various fields, flexibility to coat substrates of any size and over large areas. In this work, five compositions of lithium based cobalt ferrites *viz.* (i) $Li_{0.75}Co_{0.625}Fe_2O_4$ (ii) $Li_{0.75}Co_1Fe_{1.75}O_4$ (iii) $Li_{0.75}Co_{1.375}Fe_{1.5}O_4$ (iv) $Li_{0.75}Co_{1.75}Fe_{1.25}O_4$ and (v) $Li_{0.75}Co_{2.125}Fe_1O_4$ were synthesized using the sol-gel method. Our goal is to investigate the enhancement of electrical properties in these magnetic nanomaterials.

EXPERIMENTAL

The precursors for the synthesis of hybrid polymer matrix composite material consisted of lithium nitrate ($LiNO_3$), cobalt(II) sulphate heptahydrate ($CoSO_4{\cdot}7H_2O$), iron(III) sulphate pentahydrate ($Fe_2(SO_4)_3{\cdot}5H_2O$) and citric acid ($C_6H_8O_7$) serving as the binding agent. All the chemicals and reagents were obtained from Sigma-Aldrich Company and used without additional treatment.

Characterization: The X-ray difractometer (Xpert PRO MPD) was used to analyze the XRD patterns of cobalt lithium ferrite (LCF) using Cu*K*α radiation. The FTIR spectral analysis was conducted with Shimadzu, IRAffinity-1S at the 4000–400 cm^{-1} range. Morphologies and structural characteristics were determined by SEM with EDS using Qunata, FEG 250 instrument. The magnetic properties were studied usingvibrating sample magnetometer (VSM-9600M). Electrochemical performance of the nanopowders was carried out using CV (model: CHI Instrument-CHI1100A).

Synthesis: For the preparation of lithium cobalt ferrites (LCFs), the stoichiometric amounts of $LiNO_3$, $CoSO_4{\cdot}7H_2O$, $Fe_2(SO_4)_3{\cdot}5H_2O$ and $C_6H_8O_7$ were accurately measured and dissolved separately in distilled water to achieve a homogeneous solution. The solutions were then combined in a beaker and subjected to rigorous mixing on a magnetic stirrer for 2 h at 80 ºC, resulting in the formation of a brown gel. The gel was then dried in a hot air oven at 200 ºC for 1 h, followed by calcination at 900 ºC for 5 h in a muffle furnace. The resulting nanopowder was then ground and refined through a rigorous 2 h pestle crushing process to produce a fine powder. This process yielded the desired end product. Utilizing the same procedure, the other nanopowders of LCFs like (i) $Li_{0.75}Co_{0.625}Fe_2O_4$, (ii) $Li_{0.75}Co_1Fe_{1.75}O_4$, (iii) $Li_{0.75}Co_{1.375}Fe_{1.5}O_4$, (iv) $Li_{0.75}Co_{1.75}Fe_{1.25}O_4$ and (v) $Li_{0.75}Co_{2.125}Fe_1O_4$ were prepared.

RESULTS AND DISCUSSION

The crystalline properties of the prepared lithium cobalt ferrites (LCFs) were investigated using X-ray diffraction (XRD) offering valuable information on the crystal arrangement and particle spacing. As depicted in Fig. 1, the XRD patterns display sharp, well-defined peaks with no detectable impurities, verifying the high purity of the synthesized compounds. The P-XRD pattern of (i) $Li_{0.75}Co_{0.625}Fe_2O_4$, (ii) $Li_{0.75}Co_1Fe_{1.75}O_4$ and (iii) $Li_{0.75}Co_{1.375}Fe_{1.5}O_4$ compounds reveals a cubic structure, corresponding to the $Fd\bar{3}m$ space group. The lattice parameters interfacial length were determined as a = b = c = 8.351 (Å), 8.38 (Å), 8.384 (Å) with interfacial angles α = β = γ = 90º. The calculated volume of the cell is 582.3921(10^6pm^3), 588.48 (10^6pm^3), 589.324(10^6pm^3) and the obtained crystallite size are 36.17, 60.73, 53.3 nm, respectively. The significant peak shifts were observed at multiple miller indices with the (311) plane exhibiting the most significant change. The XRD analysis revealed that $Li_{0.75}Co_1Fe_{1.75}O_4$ (iv) and $Li_{0.75}Co_{2.125}Fe_1O_4$ (v) exhibits a cubic structure belonging to the *P*4332 and $Pm\bar{3}m$ space group with the axial length a = b = c = 8.341 (Å), 8.3296 (Å) and interfacial angles α = β = γ = 90º. The obtained cell volume are 580.302(10^6pm^3), 577.926(10^6pm^3) and the calculated crystallite sizes are 34.67 and 19.39. The lattice parameters, cell volumes and crystal sizes were computed using Scherrer's equation. Overall, it is evident that $Li_{0.75}Co_{2.125}Fe_1O_4$ (v) exhibits a lattice constant value of a = b = c = 8.3296 (Å), a cell volume of 577.926(10^6pm^3), and the smallest crystallite size at 19.39 when compared to other compounds. This reduction in results indicates that $Li_{0.75}Co_{2.125}Fe_1O_4$ (v) is denser, size and shape of the particles are more well-defined than those of the other compounds. The results are given in Table-1.

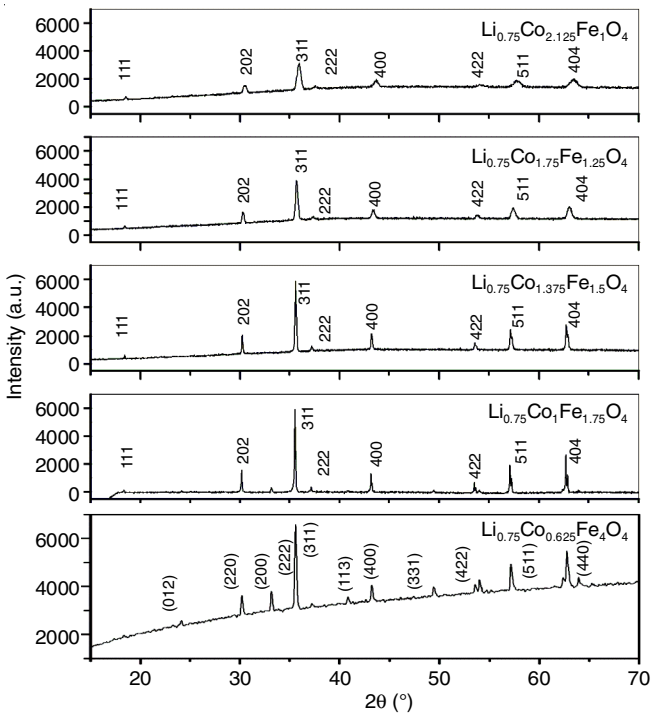

Fig. 1. XRD diffraction patterns of lithium cobalt ferrites (LCFs)

FESEM-EDS studies: Fig. 2a-e show the FESEM micrographs of $Li_{0.75}Co_{0.625}Fe_{2-x}O_4$ (y = 0.0, 0.25, 0.5, 0.75 and 1) prepared through the sol-gel method at room temperature. The images exhibit distinct nanoscale features and morphological modifications in the LCFs at varying compositions. The compositional analysis (EDS) reveals that the synthesized ferrites exhibit stochiometric ratios and devoid of impurities. The observed porosity is attributed to gas release during the synthesis process.

FTIR studies: The FT-IR spectra (Fig. 3) of the prepared $Li_{0.75}Co_{0.625}Fe_{2-x}O_4$ (y = 0.0, 0.25, 0.5, 0.75 and 1) exhibit the characteristic peaks at 389.62 cm^{-1}, 366.48 cm^{-1}, 356.83 cm^{-1}, 385.76 cm^{-1}, 370.33 cm^{-1}, 351.04 cm^{-1} and 368.40 cm^{-1} which

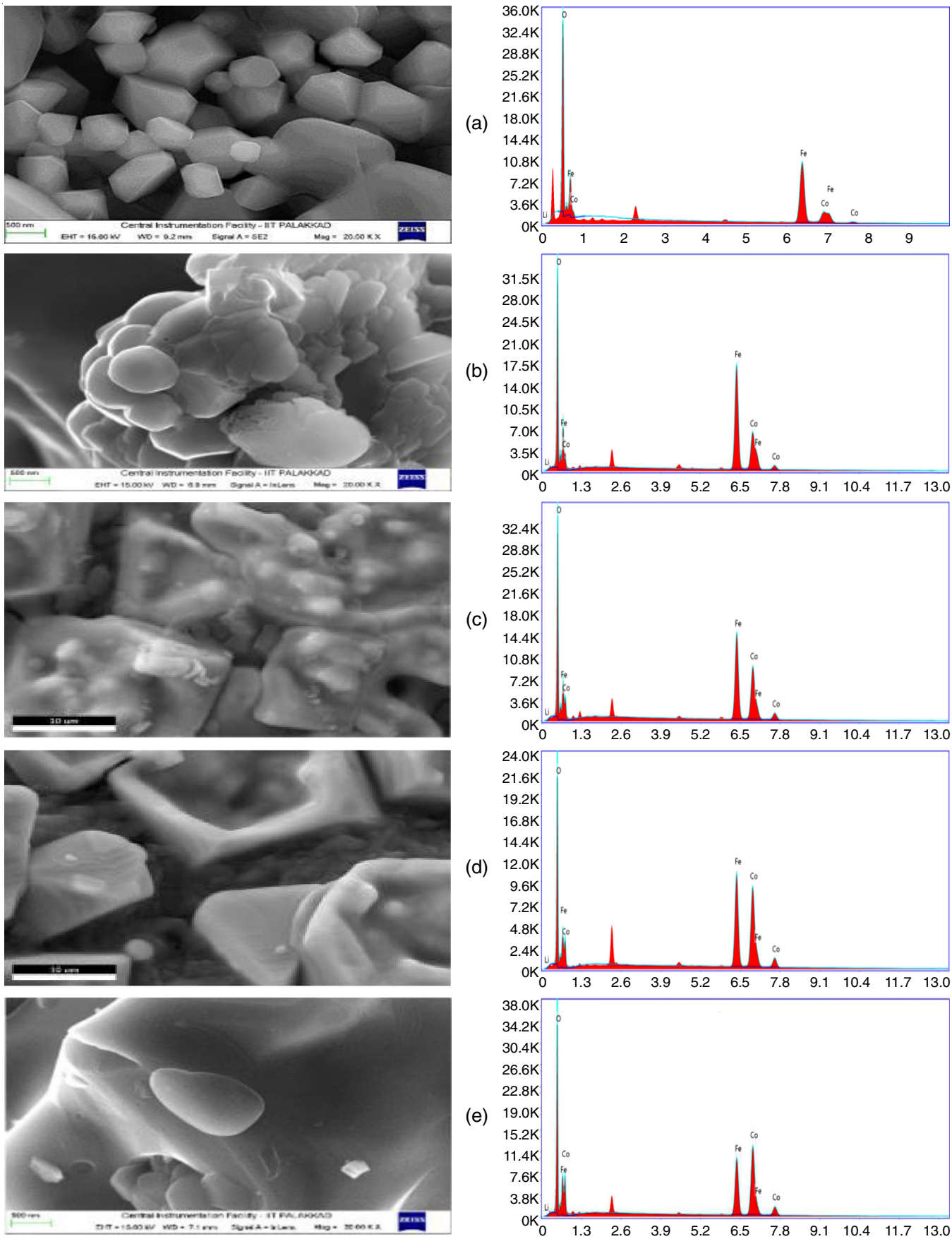

Fig. 2. EDS spectrum for (a) $Li_{0.75}Co_{0.625}Fe_{2-x}O_4$ ($y = 0.0$), (b) $Li_{0.75}Co_1Fe_{1.75}O_4$ ($y = 0.25$), (c) $Li_{0.75}Co_{1.375}Fe_{1.5}O_4$ ($y = 0.5$), (d) $Li_{0.75}Co_{1.75}Fe_{1.25}O_4$ ($y = 0.75$) and (e) $Li_{0.75}Co_{2.125}Fe_1O_4$ compound

TABLE-1
CRYSTAL STRUCTURE, LATTICE CONSTANT, UNIT CELL VOLUME AND CRYSTALLITE SIZE OF LCF COMPOUNDS

Compound	Structure	Lattice constant *a* (Å)	Unit cell volume $(Å)^3$	Crystallite size
$Li_{0.75}Co_{0.625}Fe_2O_4$	Cubic	8.351	590.99(10^6pm^3)	36.17
$Li_{0.75}Co_1Fe_{1.75}O_4$	Cubic	8.380	588.48(10^6pm^3)	60.73
$Li_{0.75}Co_{1.375}Fe_{1.5}O_4$	Cubic	8.384	589.32(10^6pm^3)	53.30
$Li_{0.75}Co_{1.75}Fe_{1.25}O_4$	Cubic	8.341	580.30(10^6pm^3)	34.67
$Li_{0.75}Co_{2.125}Fe_1O_4$	Cubic	7.696	455.80(10^6pm^3)	19.39

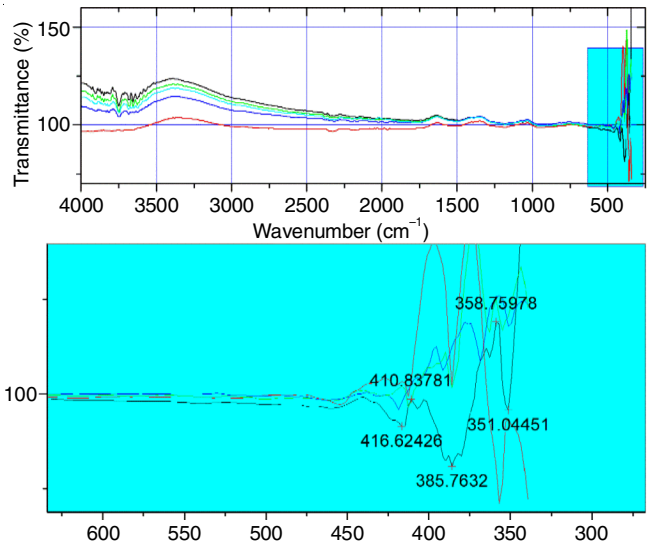

Fig. 3. FTIR analysis for (i) $Li_{0.75}Co_{0.625}Fe_{2x}O_4$, (ii) $Li_{0.75}Co_1Fe_{1.75}O_4$, (iii) $Li_{0.75}Co_{1.375}Fe_{1.5}O_4$, (iv) $Li_{0.75}Co_{1.75}Fe_{1.25}O_4$ and (v) $Li_{0.75}Co_{2.125}Fe_1O_4$

are indicative of metal-oxygen bonds (Fe-O, Co-O) confirming the presence of lithium cobalt ferrite.

Electrochemical studies: Electrochemical impedance spectroscopy (EIS) is used to analyze the electrochemical properties of materials and interfaces. The EIS data is typically presented in the form of Nyquist plots and Bode plots. For $y = 0.5$, a lower Warburg impedance suggests better ion diffusion characteristics (Figs. 4 and 5). Impedance magnitude trends offer insights into capacitive and resistive behaviours. Lower impedance magnitude at high frequencies and a phase angle closer to -90º indicate better capacitive behaviour. Due to its low charge transfer resistance, low ion diffusion and favourable impedance and phase angle values, the LCF ($y = 0.75$) performs best electrochemically.

Magnetic properties: In present study, the magnetic properties of LCFs using vibrating sample magnetometer (VSM) were analyzed. The M-H loops reveal key magnetic parameters like saturation magnetization (M_s), coercive field (H_c), remanent magnetization (M_r), squareness value (M_r/M_s), nucleation field

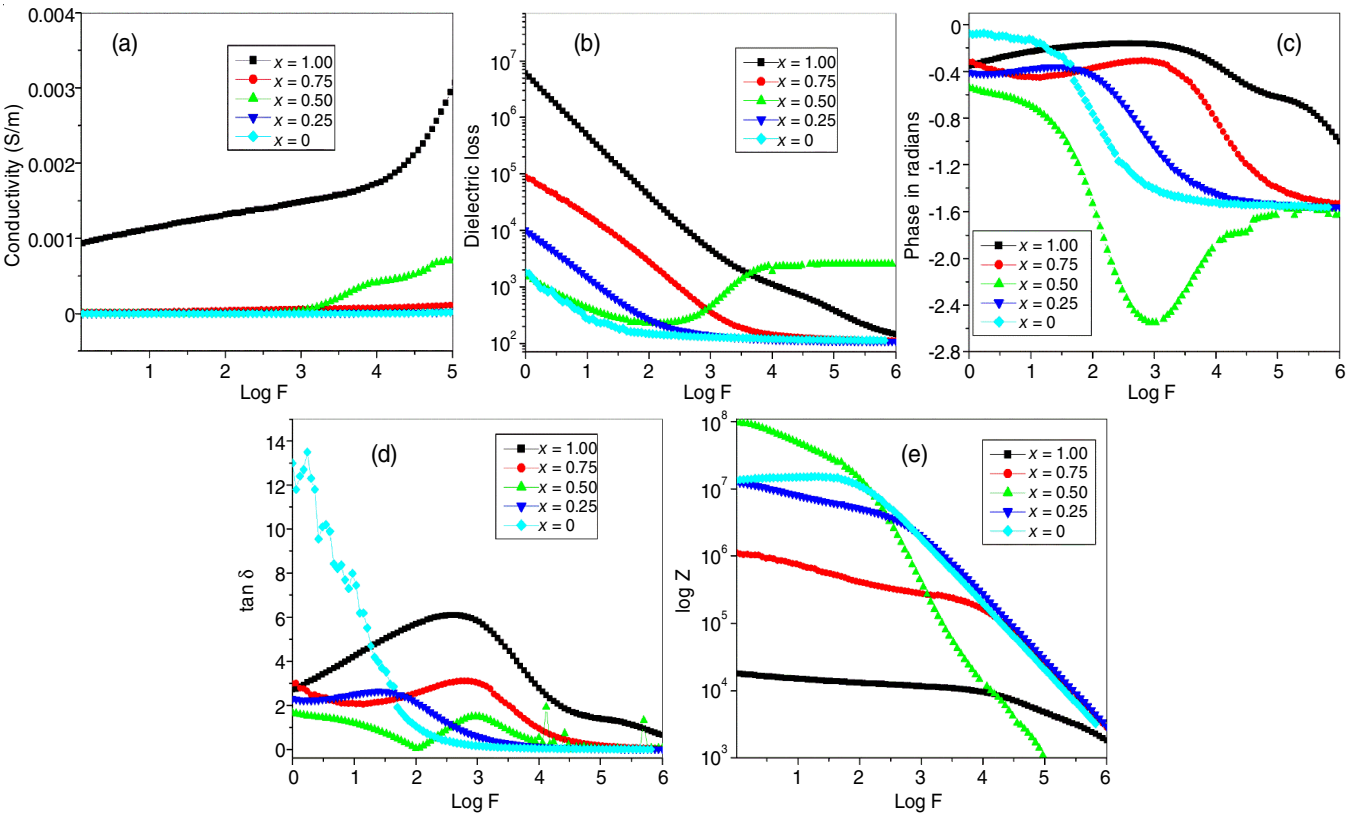

Fig 4. (a) Variation of conductivity with frequency, (b) variation of dielectric loss with frequency, (c) phase angle *vs.* log f plot, (d) variation of tan δ with frequency. (e) impedance *vs.* log f plot for (i) $Li_{0.75}Co_{0.625}Fe_2O_4$, (ii) $Li_{0.75}Co_1Fe_{1.75}O_4$, (iii) $Li_{0.75}Co_{1.375}Fe_{1.5}O_4$, (iv) $Li_{0.75}Co_{1.75}Fe_{1.25}O_4$, (v) $Li_{0.75}Co_{2.125}Fe_1O_4$, respectively

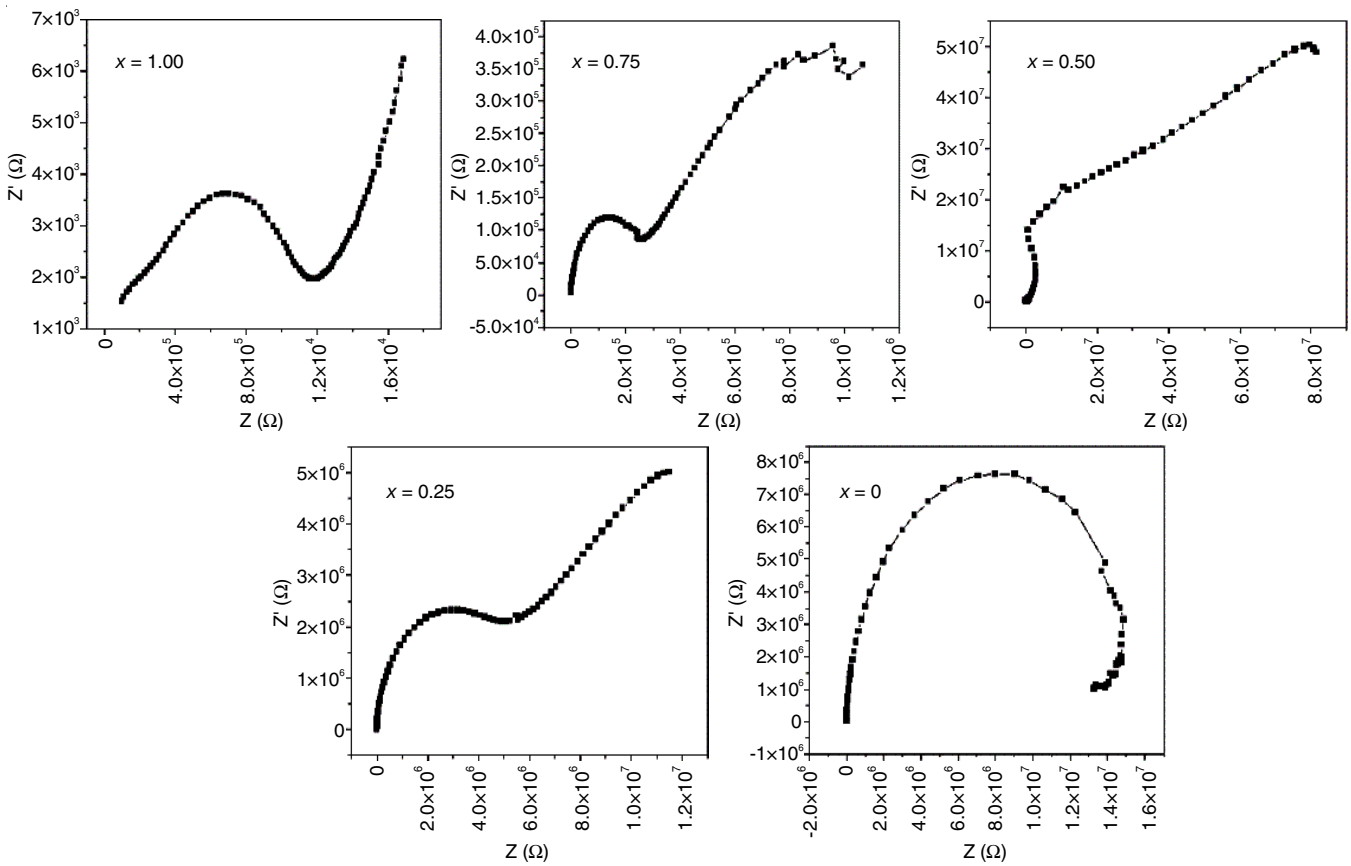

Fig 5. Nyquist plot at room temperature for (i) $Li_{0.75}Co_{0.625}Fe_2O_4$, (ii) $Li_{0.75}Co_1Fe_{1.75}O_4$, (iii) $Li_{0.75}Co_{1.375}Fe_{1.5}O_4$, (iv) $Li_{0.75}Co_{1.75}Fe_{1.25}O_4$, (v) $Li_{0.75}Co_{2.125}Fe_1O_4$

(H_n) and maximum energy loss (BH_{max}). The magnetization *versus* applied field plots *i.e.* M-H plots for the prepared LCF compounds under investigation were recorded at room temperature and also the values of these Hysteresis parameters (Fig. 6).

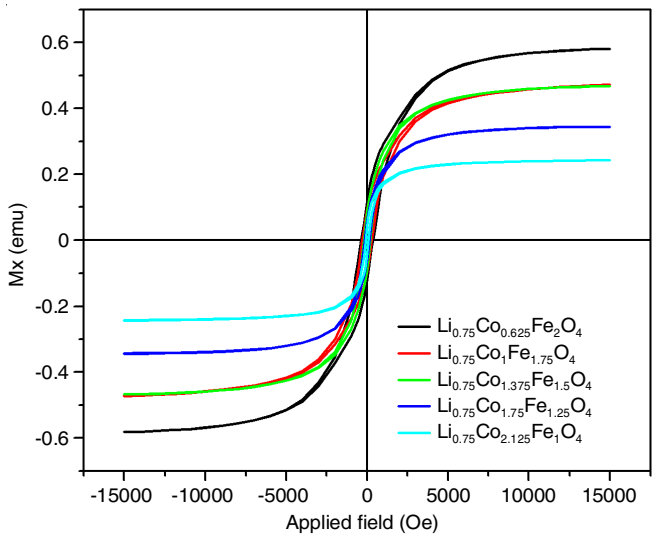

Fig. 6. M-H loop for LCF (i) $Li_{0.75}Co_{0.625}Fe_2O_4$, (ii) $Li_{0.75}Co_1Fe_{1.75}O_4$, (iii) $Li_{0.75}Co_{1.375}Fe_{1.5}O_4$, (iv) $Li_{0.75}Co_{1.75}Fe_{1.25}O_4$ and (v) $Li_{0.75}Co_{2.125}Fe_1O_4$

The coercive field (H_c) values for the synthesized ferrites range from -1.000 to -2.500, indicating they are soft magnetic materials. These materials exhibit low coercivity, enabling easy magnetization and demagnetization, high magnetic susceptibility and low remanence, suggesting the minimal retention of magnetization when the external field is withdrawn (Table-2). They have low magnetic stability *i.e.* the magnetic state is not stable and can be easily changed by external magnetic fields. Also have high susceptibility *i.e.* the material is highly responsive to magnetic fields and can be easily magnetized by weak fields. Their remanence is low, meaning the material does not hold significant magnetization after the external field has been removed, making them unsuitable for data storage. Specifically, materials with $H_c < 1$ cannot effectively maintain the magnetic information, which is critical for applications such as hard drives. However, such materials may be suitable for other applications like magnetic shielding, magnetic sensors, or transformers, where high magnetic permeability and low coercivity are beneficial.

Based on the obtained values, the LCFs ($y = 0.25$ and 1) has the highest coercive field -2.500. This value indicates a higher resistance to demagnetization, higher magnetic stability, better resistance to magnetic field changes and improved performance in applications with varying magnetic fields. The lowest coercive field is -1.000 at LCF ($y = 0.5$) and this value signifies a diminished resistance to demagnetization, decreased magnetic stability, increased susceptibility to fluctuations in magnetic fields and a possibility of compromised performance in scenarios involving variable magnetic fields. In general, on comparing all the synth-

TABLE-2
HYSTERESIS PARAMETER COMPARISON FOR (i) $Li_{0.75}Co_{0.625}Fe_{2-x}O_4$ (y = 0.0), (ii) $Li_{0.75}Co_1Fe_{2-x}O_4$ (y = 0.25), (iii) $Li_{0.75}Co_{1.375}Fe_{2-x}O_4$ (y = 0.5), (iv) $Li_{0.75}Co_{1.25}Fe_{2-x}O_4$ (y = 0.75) AND (v) $Li_{0.75}Co_{2.125}Fe_{2-x}O_4$ (y = 1) COMPOUNDS

Compounds	Coercive field H_c (Oe)	Remanent magnetization $M_r \times 10^{-3}$ emu	Squareness M_r/Ms	1-(M_r/H_c) (1/slope at H_c)	H_c offset (Oe)	Saturation field H_s (Oe)	Nucleation field H_n (Oe)	Maximum energy loss BH_{max} MGs (Oe)
LCF (y = 0)	-2.000	117.103	0.419	1.148	-15004.0	8934.63	8580.30	640.939
LCF (y = 0.25)	-2.500	93.831	0.394	1.146	-15003.5	8931.77	8469.40	479.544
LCF (y = 0.50)	-1.000	85.449	0.330	1.131	-15002.0	8461.64	8308.01	509.719
LCF (y = 0.75)	-2.000	58.394	0.288	1.119	-15003.0	8386.64	8270.52	335.117
LCF (y = 1.00)	-2.500	41.831	0.264	1.112	-15003.5	8245.61	7982.44	182.784

esized compounds H_c values, materials with higher coercive fields of LCFs (y = 0.25 and 1) are suitable for the applications requiring strong magnetic fields, such as permanent magnets, magnetic resonance imaging, electric motors and generators.

The remanent magnetization (M_r) values for the synthesized LCFs decrease with increasing y, ranging from 117.103 $\times 10^{-3}$ (for y = 0) to 41.831 $\times 10^{-3}$ (for y = 1). The ferrites with y = 0 exhibits the highest M_r indicating stronger magnetic field retention, better magnetic performance and higher efficiency in various applications. The squareness (M_r/M_s) values of LCFs decrease from 0.419 to 0.264 as the amount of y increases, all remaining below 0.5. This indicates the low remanence, gradual magnetic response with non-square hysteresis loops and unsuitability for permanent magnet applications requiring strong magnetic remanence. However, such materials are well-suited for soft magnetic applications, including magnetic sensors, actuators and MRI technologies, where a soft magnetic response and low hysteresis are advantageous.

The synthesized LCFs (y = 0, 0.25, 0.5, 0.75, 1) exhibit average coercive field (H_c) values of -15004.0, -15003.50, -15002.00, -15003.00 and -15003.50 Oe, indicating consistent magnetization behaviour. The negative H_c values reflect ferrimagnetic or antiferromagnetic characteristics, with minimal variation (2 Oe) across samples. This consistency suggests robust magnetic property measurements and a low coercive field, making these materials ideal for applications requiring easy magnetization and demagnetization, such as magnetic sensors, actuators or MRI technologies. Similarly, the saturation field (H_s) values obtained for LCFs (y = 0, 0.25, 0.5, $_{0.75}$ and 1) are found to be 8934.63, 8931.77, 8461.64, 8386.64 and 8245.61. These values are quite close, with a relatively small range of approximately 700 Oe (from 8245.61 to 8934.63). This suggests that the material's saturation field is relatively consistent with the minimal variation. Overall, these values indicate a material with a relatively high saturation field, which suggests higher magnetic stability, greater resistance to demagnetization and potential for applications in the stronger magnetic fields.

The nucleation field (H_n) values obtained for synthesized LCFs (y = 0, 0.25, 0.5, $_{0.75}$ and 1) are 8580.30, 8469.40, 8308.10, 8270.52 and 7982.44. A higher nucleation field for LCF (y = 0) indicates a material with higher magnetic coercivity, greater resistance to magnetization reversal and higher magnetic stability. The maximum energy loss (BH_{max}) parameter characterizes the magnetic properties of a material. It represents the maximum energy loss (MGOe) which occurs when the material is magnetized and demagnetized. The maximum energy loss for the synthesized LCFs (y = 0, 0.25, 5, 0.75 and 1) values are -640.939, -479.544, -509.719, -335.117 and -182.784. On comparing the BH_{max} values, the lowest BH_{max} value of LCFs (y = 0.75 & 1) -182.784 is the best in terms of energy efficiency and magnetic performance.

Conclusion

A comparative XRD analysis of the synthesized lithium cobalt ferrites (LCFs) (y = 0, 0.25, 0.5, 0.75 and 1) prepared by sol-gel based method revealed the distinct cubic structures with varying space groups. The lattice constant of $Li_{0.75}Co_{(5+3x/8)}Fe_{2-y}O_4$ (y = 1) is the lowest at 7.696 Å indicating the higher density due to the compact atomic arrangements, stronger interatomic bonding, enhancing hardness and resistance to deformation, elevated melting points and superior thermal conductivity potential. The crystallite size of 19.39 nm for y = 1 suggests nanoscale dimensions with increased surface area, enhanced mechanical properties and possible quantum confinement effects, yielding unique physical attributes. The morphological studies *via* FESEM confirm the nanoscale nature of the synthesized compounds, while EDS spectra confirmed the presence of Li, Fe and O elements. Due to its low atomic number, Li remains undetectable in FESEM. The absence of impurities or precursors indicates high purity. FTIR analysis highlights metal-oxygen bond peaks (Fe-O, Co-O) around 350 cm^{-1}, affirming the presence of lithium cobalt ferrite. The VSM analysis confirms all compounds exhibit coercivity values below 1 Oe ($H_c < 1$), classifying them as soft magnetic materials. Among the samples, LCF (y = 0) demonstrates the highest remanent magnetization (117.103 $\times 10^{-3}$ emu), while LCF (y = 1) has the lowest (41.831 $\times 10^{-3}$ emu). The loop squareness ratio (M_r/Ms) below 0.5 across all samples signifies a multi-domain magnetic particle nature. Furthermore, the y = 1 composition exhibits the minimal saturation and nucleation fields with lower energy loss compared to others. Electrochemical analysis reveals LCF (y = 1) exhibits superior performance due to minimal charge transfer resistance, enhanced ion diffusion, optimal impedance, phase angle characteristics and excellent capacitive performance. As a soft magnetic material with negative coercivity, low remanent magnetization, high conductivity and reduced dielectric loss at elevated frequencies, this compound provides significant advantages for lithium-ion battery applications.

CONFLICT OF INTEREST

The authors declare that there is no conflict of interests regarding the publication of this article.

REFERENCES

1. N. Baig, I. Kammakakam and W. Falath, *Mater. Adv.*, **2**, 1821 (2021); https://doi.org/10.1039/D0MA00807A
2. H.M. Saleh and A.I. Hassan, *Sustainability*, **15**, 10891 (2023); https://doi.org/10.3390/su151410891
3. L. Pokrajac, A. Abbas, W. Chrzanowski, G.M. Dias, B.J. Eggleton, S. Maguire, E. Maine, T. Malloy, J. Nathwani, L. Nazar, A. Sips, J. Sone, A. van den Berg, P.S. Weiss and S. Mitra, *ACS Nano*, **15**, 18608 (2021); https://doi.org/10.1021/acsnano.1c10919
4. C.A. Charitidis, P. Georgiou, M.A. Koklioti, A.-F. Trompeta and V. Markakis, *Manufacturing Rev.*, **1**, 11 (2014); https://doi.org/10.1051/mfreview/2014009
5. A. Mittal, I. Roy and S. Gandhi, *Magnetochemistry*, **8**, 107 (2022); https://doi.org/10.3390/magnetochemistry8090107
6. S.G. Divakara and B. Mahesh, *Results Eng.*, **21**, 101702 (2024); https://doi.org/10.1016/j.rineng.2023.101702
7. N. Maji and H.S. Dosanjh, *Magnetochemistry*, **9**, 156 (2023); https://doi.org/10.3390/magnetochemistry9060156
8. K.K. Kefeni, T.A.M. Msagati and B.B. Mamba, *Mater. Sci. Eng. B*, **215**, 37 (2017); https://doi.org/10.1016/j.mseb.2016.11.002
9. B. Issa, I.M. Obaidat, B.A. Albiss and Y. Haik, *Int. J. Mol. Sci.*, **14**, 21266 (2013); https://doi.org/10.3390/ijms141121266
10. N.J. Mondal, R. Sonkar, B. Boro, M.P. Ghosh and D. Chowdhury, *Nanoscale Adv.*, 5, 5460 (2023); https://doi.org/10.1039/D3NA00446E
11. S.F. Mansour and M.A. Elkestawy, *Ceram. Int.*, **37**, 1175 (2011); https://doi.org/10.1016/j.ceramint.2010.11.038
12. K. Poon and G. Singh, *ChemNanoMat*, **10**, e202400168 (2024); https://doi.org/10.1002/cnma.202400168
13. A.V. Trukhanov, D.I. Tishkevich, A.V. Timofeev, V.A. Astakhov, E.L. Trukhanova, A.A. Rotkovich, Yuan Yao, D.S. Klygach, T.I. Zubar, M.I. Sayyed, S.V. Trukhanov and V.G. Kostishin, *Ceram. Int.*, **50**, 21311 (2024); https://doi.org/10.1016/j.ceramint.2024.03.241
14. T.N. Pham, T.Q. Huy and A.-T. Le, *RSC Adv.*, **10**, 31622 (2020); https://doi.org/10.1039/D0RA05133K
15. N. Askarzadeh and H. Shokrollahi, *Results Chem.*, **10**, 101679 (2024); https://doi.org/10.1016/j.rechem.2024.101679
16. R.S. Rajenimbalkar, V.J. Deshmukh, K.K. Patankar and S.B. Somvanshi, *Sci. Rep.*, **14**, 29547 (2024); https://doi.org/10.1038/s41598-024-81222-3
17. E.E. Ateia, M.A. Ateia, M.G. Fayed, S.I. El-Hout, S.G. Mohamed and M.M. Arman, *Appl. Phys. A*, **128**, 483 (2022); https://doi.org/10.1007/s00339-022-05622-w
18. N. Jovic, B. Antic, G.F. Goya and V. Spasojevic, *Curr. Nanosci.*, **8**, 651 (2012); https://doi.org/10.2174/157341312802884391
19. S. Aman, M.B. Tahir and N. Ahmad, *J. Mater. Sci.: Mater. Electron.*, **32**, 22440 (2021); https://doi.org/10.1007/s10854-021-06730-8
20. J.A. Goudar, S.N. Thrinethra, S. Chapi, M.V. Murugendrappa, M.R. Saeb and M. Salami-Kalajahi, *Adv. Energy Sustain. Res.*, **6**, 2400271 (2025); https://doi.org/10.1002/aesr.202400271
21. S. Rasheed, H.S. Aziz, R.A. Khan, A.M. Khan, A. Rahim, J. Nisar, S.M. Shah, F. Iqbal and A.R. Khan, *Ceramics Int.*, **42**, 3666 (2016); https://doi.org/10.1016/j.ceramint.2015.11.034
22. M.K. Shobana, *J. Phys. Chem. Solids*, **73**, 1040 (2012); https://doi.org/10.1016/j.jpcs.2012.03.009
23. S.E. Shirsath, D. Wang, S.S. Jadhav, M.L. Mane and S. Li, in eds.: L. Klein, M. Aparicio and A. Jitianu, Ferrites obtained by Sol-Gel Method. Handbook of Sol-Gel Science and Technology. Springer, Cham (2018); https://doi.org/10.1007/978-3-319-19454-7_125-3
24. Y. Cao, H. Qin, X. Niu and D. Jia, *Ceram. Int.*, **42**, 10697 (2016); https://doi.org/10.1016/j.ceramint.2016.03.184
25. A.V. Vinogradov and V.V. Vinogradov, *RSC Adv.*, **4**, 45903 (2014); https://doi.org/10.1039/C4RA04454A